

identified as inhibitory for heart field specification (19, 20).

To determine whether Wnt signaling is required to promote PC fate, we microinjected cells expressing the soluble Wnt antagonist Crescent (19, 20) adjacent to PC precursors before their specification. After 8 hours, PC precursors were explanted and allowed to differentiate *ex vivo*. Exposure to Crescent decreased the slope of PC phase 4 depolarization by 65% relative to control injections (Fig. 4, B and D). These experiments could not rule out the possibility that Crescent is interacting with factors not associated with canonical Wnt signaling. Therefore, to further demonstrate that Wnt signaling was capable of inducing PC fate, we injected Wnt-expressing cells into the presumptive heart fields. This resulted in a 69% increase in phase 4 slope (Fig. 4, C and D). We then used Bio, a pharmacological inhibitor of glycogen synthase kinase 3 (GSK3) that has been shown to stabilize β -catenin (21, 22) to activate Wnt signaling in the heart field. Consistent with the findings above, 10 μ M Bio increased diastolic slope in heart field explants relative to control cells (fig. S10).

When we allowed injected embryos to develop to late looping stages, aberrant Wnt signaling led to severe morphological defects, consistent with previous reports (Fig. 4, F and H) (23). Crescent injection adjacent to PC precursors led to the ectopic expression of Nkx2.5 in PC at St18, which is in agreement with a conversion of PC into a more working myocardial fate (24) (Fig. 4, E and F). About 35% of Wnt-injected embryos survived to heart looping stages. Wnt introduction into the primary and secondary heart field mesoderm resulted in irregularly contracting hearts, with decreased Nkx2.5 expression on the injected

side of the embryo (Fig. 4, G and H). To confirm that these Nkx2.5-negative regions were still electrically active, we performed optical mapping. Consistent with a Wnt-based conversion of working myocardium into PC-like cells, we detected retrograde propagation (outflow toward inflow) as well as ectopic pacemaker sites (movie S8). These ectopic sites were restricted to the Wnt-injected side of the embryo and displayed AP shapes similar to those of control PCs (Fig. 4, I and J, and movie S8).

These findings suggest that early mesodermal Wnt-mediated cues are sufficient to induce pacemaker-like fates that do not manifest until late looping stages. However, Wnts are broadly and bilaterally expressed in the posterior mesoderm, so it is likely that additional cues are required to restrict PC fate, including laterality genes (25, 26). The early diversification of PC fate from the working myocardium suggests that fate specification is assigned directly in the lateral plate mesoderm, and is not the result of the specialization of an already functional embryonic myocyte. These data establish a framework through which PC development should be viewed, thereby providing a foundation for tissue engineering and stem cell-based approaches for PC generation.

References and Notes

1. A. Keith, M. Flack, *J. Anat. Physiol.* **41**, 172 (1907).
2. E. C. Hoff, T. C. Kramer, D. DuBois, B. M. Patten, *Am. Heart J.* **17**, 470 (1939).
3. L. H. S. Van Mierop, *Am. J. Physiol.* **212**, 407 (1967).
4. K. Kamino, A. Hirota, S. Fujii, *Nature* **290**, 595 (1981).
5. M. Buckingham, S. Meilhac, S. Zaffran, *Nat. Rev. Genet.* **6**, 826 (2005).
6. V. Hamburger, H. L. Hamilton, *J. Morphol.* **88**, 49 (1951).

7. M. Lieberman, A. Paes de Carvalho, *J. Gen. Physiol.* **49**, 351 (1965).
8. J. Stieber *et al.*, *Proc. Natl. Acad. Sci. U.S.A.* **100**, 15235 (2003).
9. T. M. Vinogradova *et al.*, *Circ. Res.* **107**, 767 (2010).
10. K. Y. Bogdanov, T. M. Vinogradova, E. G. Lakatta, *Circ. Res.* **88**, 1254 (2001).
11. M. E. Rawles, *Physiol. Zool.* **16**, 22 (1943).
12. H. Stalsberg, R. L. DeHaan, *Dev. Biol.* **19**, 128 (1969).
13. R. Abu-Issa, M. L. Kirby, *Dev. Biol.* **319**, 223 (2008).
14. T. J. Lints, L. M. Parsons, L. Hartley, I. Lyons, R. P. Harvey, *Development* **119**, 419 (1993).
15. I. Lyons *et al.*, *Genes Dev.* **9**, 1654 (1995).
16. S. Yuan, G. C. Schoenwolf, *Anat. Rec.* **260**, 204 (2000).
17. C. L. Cai *et al.*, *Dev. Cell* **5**, 877 (2003).
18. Q. Ma, B. Zhou, W. T. Pu, *Dev. Biol.* **323**, 286 (2008).
19. M. J. Marvin, G. Di Rocco, A. Gardiner, S. M. Bush, A. B. Lassar, *Genes Dev.* **15**, 316 (2001).
20. V. A. Schneider, M. Mercola, *Genes Dev.* **15**, 304 (2001).
21. L. Meijer *et al.*, *Chem. Biol.* **10**, 1255 (2003).
22. N. Sato, L. Meijer, L. Skaltsounis, P. Greengard, A. H. Brivanlou, *Nat. Med.* **10**, 55 (2004).
23. S. M. Maniasty, M. Han, K. K. Linask, *Dev. Dyn.* **235**, 2160 (2006).
24. M. T. Mommersteeg *et al.*, *Circ. Res.* **100**, 354 (2007).
25. J. Wang *et al.*, *Proc. Natl. Acad. Sci. U.S.A.* **107**, 9753 (2010).
26. G. Ammirabile *et al.*, *Cardiovasc. Res.* **93**, 291 (2012).

Acknowledgments: We thank T. Kornberg, D. Stainier, S. Coughlin, and R. Shaw for their comments, and Mikawa lab members for their suggestions. All data reported in this paper can be found in the main text or supplementary materials. Supported by NIH grants R01HL093566 and R01HL112268 (T.M.) and T32HL007544 (M.B.).

Supplementary Materials

www.sciencemag.org/cgi/content/full/science.1232877/DC1
Materials and Methods
Figs. S1 to S10
Tables S1 and S2
Movies S1 to S8
References (27, 28)

19 November 2012; accepted 13 March 2013
Published online 21 March 2013;
10.1126/science.1232877

Wolbachia Invades *Anopheles stephensi* Populations and Induces Refractoriness to *Plasmodium* Infection

Guowu Bian,^{1,2} Deepak Joshi,¹ Yuemei Dong,³ Peng Lu,¹ Guoli Zhou,¹ Xiaoling Pan,¹ Yao Xu,¹ George Dimopoulos,³ Zhiyong Xi^{1,4*}

Wolbachia is a maternally transmitted symbiotic bacterium of insects that has been proposed as a potential agent for the control of insect-transmitted diseases. One of the major limitations preventing the development of *Wolbachia* for malaria control has been the inability to establish inherited infections of *Wolbachia* in anopheline mosquitoes. Here, we report the establishment of a stable *Wolbachia* infection in an important malaria vector, *Anopheles stephensi*. In *A. stephensi*, *Wolbachia* strain *wAlbB* displays both perfect maternal transmission and the ability to induce high levels of cytoplasmic incompatibility. Seeding of naturally uninfected *A. stephensi* populations with infected females repeatedly resulted in *Wolbachia* invasion of laboratory mosquito populations. Furthermore, *wAlbB* conferred resistance in the mosquito to the human malaria parasite *Plasmodium falciparum*.

The ability of *Wolbachia* to spread through cytoplasmic incompatibility (CI) (1, 2) and render mosquitoes resistant to a variety of human pathogens (3–6) has instigated the development of *Wolbachia*-based strategies for both suppression and replacement of disease vec-

tor populations (2, 7). Given their medical importance, there have been considerable efforts to extend this approach to anopheline malaria vector mosquitoes, which are not naturally infected by *Wolbachia* spp. (8). Over the past two decades, various attempts to artificially generate stably in-

fecting *Anopheles* spp. have failed, raising concern that the *Anopheles* germ line is inhospitable to *Wolbachia* or that *Wolbachia* infection might cause reproductive ablation in *Anopheles* mosquitoes (6). Studies based on a transient somatic infection have recently indicated that *Wolbachia* can inhibit the development of the malaria parasite in the *Anopheles* mosquito, possibly by stimulating a mosquito antiparasitic immune response (5, 6). These results reinforced the potential of a *Wolbachia*-based intervention for malaria vector control, but only if the bacterium could be made to form a stable association with this mosquito.

Anopheles stephensi is the major vector of human malaria in the Middle East and South Asia. We

¹Department of Microbiology and Molecular Genetics, Michigan State University, East Lansing, MI 48824, USA. ²Department of Parasitology, Zhongshan School of Medicine, Key Laboratory of Tropical Disease Control, Ministry of Education, Sun Yat-Sen University, Guangzhou, Guangdong 510080, China. ³W. Harry Feinstone Department of Molecular Microbiology and Immunology, Bloomberg School of Public Health, Johns Hopkins University, 615 North Wolfe Street, Baltimore, MD 21205–2179, USA. ⁴Sun Yat-sen University—Michigan State University Joint Center of Vector Control for Tropical Diseases, Guangzhou, Guangdong 510080, China.

*Corresponding author. E-mail: xizy@msu.edu

infected *A. stephensi* [Liston strain (LIS)] by embryonic microinjection of the *wAlbB* *Wolbachia* strain derived from *Aedes albopictus* (Houston strain) (9). Cytoplasm was withdrawn from *A. albopictus* embryos and directly injected into the posterior of *A. stephensi* early embryos (1). After oviposition, we used polymerase chain reaction (PCR) to test females (G_0) developed from surviving embryos for *Wolbachia* infection. We observed a stable *wAlbB* infection in one isofemale line (designated LB1) at G_1 with a 100% infection frequency maintained through G_{34} (the last generation assayed thus far). At G_9 , G_{10} , and G_{11} , we randomly selected 20 individuals (10 males and 10 females) from the LB1 cage population and tested them by diagnostic PCR (10). All

individuals ($n = 60$) were infected with *wAlbB* (fig. S1).

The 100% maternal transmission efficiency was also confirmed by fluorescence in situ hybridization (FISH) of LB1 mosquito ovaries showing heavy *wAlbB* infection of all ovarian egg chambers. In the ovaries of the 5-day-old non-blood-fed females, *wAlbB* was mainly found in the oocytes of the egg chambers, with a low-level presence in nurse cells (Fig. 1A). This observation is consistent with a previous model showing *Wolbachia* migration from nurse cells to the oocytes through the ring canals during oogenesis (11). As in *A. albopictus* and the transinfected *Aedes aegypti* WB1 line (1, 12), *Wolbachia* was concentrated in the anterior and posterior part of LB1 mos-

quito oocytes 3 days after a blood meal (fig. S2), indicating that the *wAlbB* distribution pattern in the ovaries is conserved between mosquito species.

Of 8087 eggs resulting from crosses between LB1 males and the naturally uninfected LIS females, only 1.2% (95% confidence interval = 0.15 to 2.16) hatched (Fig. 1B), indicating a typical CI pattern. We observed a >50% egg-hatch rate in the other cross types. The egg hatches resulting from LB1 self-crosses (52.4%) were significantly lower than those observed in compatible crosses of wild-type individuals (91.0%; $P < 0.01$, $\chi^2 = 2016.4$). Outcrossing of the LB1 females with LIS males for four generations did not improve the egg-hatch rate, but tetracycline treatment of the outcrossed line increased the rate to $85.9 \pm 5.3\%$ (fig. S3), supporting the hypothesis that the *wAlbB* infection is responsible for the reduced hatch rate.

To assess the ability of the *wAlbB* infection to invade a natural uninfected population, we seeded LB1 females at ratios of 5, 10, and 20% into uninfected LIS cage populations composed of 50 females and 50 males. To promote population replacement, we also released 100 LB1 males at every generation to suppress the effective mating of LIS females. In all populations, *wAlbB* increased to 100% infection frequency within eight generations and remained fixed in subsequent generations (Fig. 1C). These results support the potential for *Wolbachia* to mediate population replacement in a public health intervention strategy. Specifically, the *wAlbB* infection was able to invade and replace the naturally uninfected cytotype within eight generations after an introduction rate as low as 5% and continued inundative release of males at a rate of two times the male population size each generation. These results also raise the challenge in application that large-scale programs for breeding and releasing male infected mosquitoes might be necessary, perhaps in conjunction with short-term intensive mosquito abatement.

A transient *Wolbachia* infection in *Anopheles gambiae* mosquitoes is known to inhibit *Plasmodium falciparum* development (5, 6). To assess the possible anti-*P. falciparum* activity of *wAlbB* in the transinfected LB1 mosquitoes, we fed them on a gametocyte culture, along with LIS

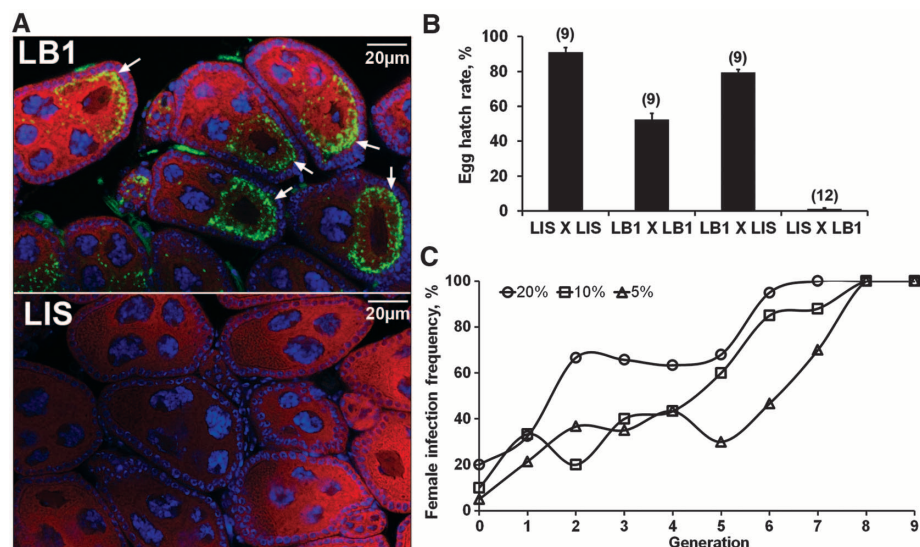
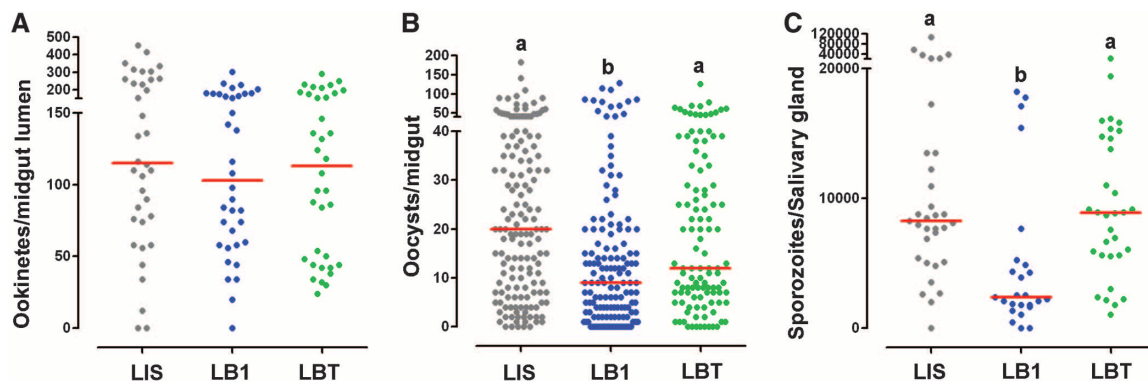


Fig. 1. Establishment and invasion of *Wolbachia wAlbB* in *A. stephensi* populations. (A) *wAlbB* distribution in the ovarian egg chambers of 5-day-old non-blood-fed LB1 females with LIS females as controls. *Wolbachia*, cytoplasm, and nuclear DNA were stained with 16S ribosomal DNA *Wolbachia* probes (green), propidium iodide (red), and 4',6-diamidino-2-phenylindole (blue), respectively. White arrows indicate *Wolbachia*. (B) *wAlbB* induces nearly complete CI in *A. stephensi* when infected males are crossed with uninfected females. Error bars indicate SE. The number of replicates for each of the four cross types is shown in parentheses. (C) *wAlbB* invades the *A. stephensi* laboratory populations. Female infection frequency was measured by PCR after a single release of LB1 females into LIS populations and continued inundative release of LB1 males at a rate of twice the male population size for each generation.

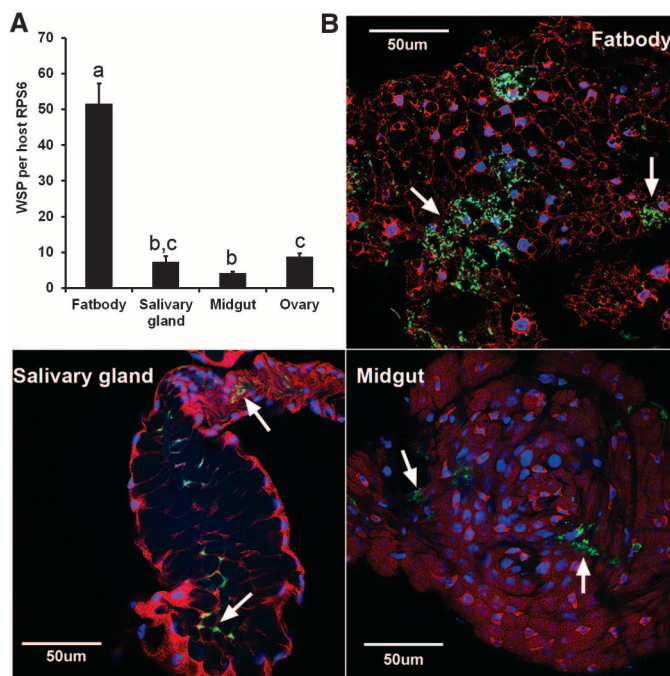
Fig. 2. *Wolbachia wAlbB*-mediated inhibition of *Plasmodium* development. *P. falciparum* ookinete (A), oocyst (B), and sporozoite (C) loads in midgut lumens, midguts, and salivary glands, respectively, of *A. stephensi* LIS, LB1, and LBT strains. Points represent the number of parasites from an individual mosquito; horizontal lines indicate the median number of parasites per tissue. Different letters above each column signify distinct statistical groups [(B) $P < 0.0001$ for LB1 versus LIS and $P < 0.01$ for LB1 versus LBT; (C) $P < 0.001$ for both LB1 versus LIS and LB1 versus LBT; Mann-Whitney test].



and the aposymbiotic line LBT mosquitoes (generated by tetracycline treatment of the LB1 strain to remove *wAlbB*) as controls. Although the presence of *wAlbB* had no impact on the ookinete stage parasites before midgut invasion (Fig. 2A and table S1), it did result in a significantly reduced prevalence and mean intensity of the oocyst stage parasite on the basal side of the midgut, as assayed at 7 days postinfection (dpi). Specifically, the LB1 strain displayed significantly lower infection prevalence and intensity than the LIS strain (Mann-Whitney U test, $P < 0.0001$) and the aposymbiotic LBT strain (Mann-Whitney U test, $P < 0.01$), whereas no difference was observed between the LIS and LBT strains (Fig. 2B and table S1). We also investigated the impact of *wAlbB* on the salivary gland sporozoite stage infection at 14 dpi and observed a greater inhibition than at the oocyst stage (Fig. 2C and table S1). *wAlbB* infection resulted in a 3.4- and 3.7-fold reduction in the sporozoite loads in salivary glands of LB1 mosquitoes when compared with LIS and LBT mosquitoes, respectively (Mann-Whitney U test, $P < 0.001$) (Fig. 2C and table S1). These data suggest that *wAlbB* inhibit *P. falciparum* development between the preinvasion luminal ookinete and oocyst stages and between the oocyst and salivary gland sporozoite stages.

A local distribution of *wAlbB* and *wMelPop* strains in mosquito somatic tissues, especially those in which pathogens replicate, develop, and travel, is important for *Wolbachia* to induce pathogen interference (4, 13). We examined the *wAlbB* density in midguts, salivary glands, and fat bodies from 7-day-old LB1 non-blood-fed females by real-time PCR. We detected *Wolbachia wAlbB* in all tissues, with a marked 5.9-fold higher density in the fat bodies than in the ovaries (Fig. 3A).

Fig. 3. *Wolbachia wAlbB* distribution in somatic tissues of LB1 mosquitoes (*G27*). (A) The genome copy of *Wolbachia* surface protein (WSP) was measured by real-time PCR and normalized by *A. stephensi* ribosomal protein S6 (RPS6). Different letters above each column signify distinct statistical groups ($P < 0.05$ for comparison between a, b, and c; Student's *t* test). Error bars indicate SEM of at least 10 biological replicates. (B) *Wolbachia wAlbB* distribution in fat body, midgut, and salivary gland of an LB1 mosquito, assayed by FISH as described in Fig. 1A. White arrows indicate *Wolbachia*.



Salivary glands and ovaries contained similar levels of *wAlbB*, whereas midguts had lower infection than ovaries, a distribution confirmed by FISH assay (Fig. 3B). This result is similar to observations made in the transiently infected *A. gambiae*, in that *Wolbachia* resided primarily within cells of the fat bodies and had a low affinity for midgut cells (6).

We have previously shown that *wAlbB* induces the production of reactive oxygen species (ROS) in *Aedes* (14), and other work has shown that ROS can inhibit *Plasmodium* infection in *Anopheles* (15, 16). To explore whether *wAlbB*-induced ROS could play a role in the mosquitoes' resistance to *Plasmodium*, we compared the levels of H_2O_2 in midguts, fat bodies, and whole bodies of LB1 and LIS mosquitoes. The levels of H_2O_2 were significantly higher in tissues of LB1 mosquitoes than in those of LIS mosquitoes (Student's *t* test, $P < 0.01$) (Fig. 4) and nearly twofold higher in whole LB1 than in LIS mosquitoes.

In conclusion, we show that the *Wolbachia wAlbB* strain can form a stable symbiosis with *A. stephensi*, invade laboratory mosquito populations through CI, and confer elevated resistance to *Plasmodium* infection, potentially through ROS generation. Previous failures in establishing a stable *Wolbachia* infection in *Anopheles* mosquitoes may be due to the *Wolbachia* strains used. To form a symbiosis, the *Wolbachia* strain should be sufficiently invasive to establish an infection in germ tissues but without being lethal to the host. The success of *wAlbB* may be attributed to its ability to confer a fitness advantage to its host (10) and its high infectivity to *Anopheles* germ tissues (17). We used a previously described embryo microinjection technique (1) but observed a lower survivor rate, possibly due to the greater sensitivity of *Anopheles* eggs to desiccation. The

low egg-hatch rate associated with the *wAlbB* infection in *A. stephensi*, which is not observed in *wAlbB*-infected *A. aegypti*, may be related to the use of mouse (an unnatural host) blood in this study. A previous study has reported suppression of egg hatch after a long-distance transfer of *wMelPop* into *A. aegypti* feeding on nonhuman blood sources, but only mild decreases when the mosquitoes fed on human blood (18).

The recent success of a field trial has demonstrated that *Wolbachia* can be deployed as a practical dengue intervention strategy, with the potential for area-wide implementation (2). The design of *Wolbachia*-based malaria control strategies would have to accommodate the fact that *Plasmodium* is vectored by multiple and frequently sympatric *Anopheles* species in different parts of the world (19, 20). However, this complication can be resolved by integrating a *Wolbachia*-based approach with other vector control strategies and by targeting the dominant malaria vectors that are the most difficult to control. For example, *Wolbachia* could be used to target outdoor-biting and -resting species that can evade current vector control methods, such as insecticide-treated nets and residual insecticide sprays (21). In our studies, we used a laboratory *P. falciparum* infection model that results in unnaturally high infection intensities, reaching a median of 20 oocysts per midgut, whereas infection levels in nature rarely exceed 2 to 3 oocysts (22). As we have shown in other studies comparing natural and laboratory infection intensities (23), it is quite likely that a stable *wAlbB* infection would confer complete refractoriness under natural field conditions. Our success in rendering *A. stephensi* resistant to *P. falciparum* by stable introduction of *wAlbB* offers a potential approach to permanently reduce the vectorial capacities of dominant malaria vectors in sub-Saharan Africa, one of the most challenging goals in current malaria vector control (21). However, it is still unknown whether *Plasmodium* will develop resistance to ROS or other *Wolbachia*-mediated inhibitory mechanisms in mosquitoes.

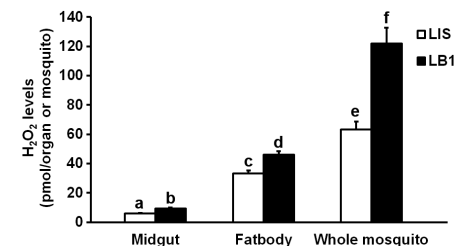


Fig. 4. *Wolbachia*-induced ROS production in LB1 mosquitoes. This figure shows a comparison of H_2O_2 levels in the fat body, midgut, and whole mosquito in 7-day-old LB1 and LIS females before a blood meal. The data shown are means of 6 (fat body and midgut) or 10 (whole-mosquito) replicates. Different letters above each column signify distinct statistical groups ($P < 0.01$ for each pair of comparison between a, b, c, d, e, and f; Student's *t* test). Error bars indicate SEM.

References and Notes

- Z. Xi, C. C. H. Khoo, S. L. Dobson, *Science* **310**, 326 (2005).
- A. A. Hoffmann *et al.*, *Nature* **476**, 454 (2011).
- G. Bian, Y. Xu, P. Lu, Y. Xie, Z. Xi, *PLoS Pathog.* **6**, e1000833 (2010).
- L. A. Moreira *et al.*, *Cell* **139**, 1268 (2009).
- Z. Kambris *et al.*, *PLoS Pathog.* **6**, e1001143 (2010).
- G. L. Hughes, R. Koga, P. Xue, T. Fukatsu, J. L. Rasgon, *PLoS Pathog.* **7**, e1002043 (2011).
- C. L. Brelsfoard, Y. Séchan, S. L. Dobson, *PLoS Negl. Trop. Dis.* **2**, e129 (2008).
- P. Kittayapong, K. J. Baisley, V. Baimai, S. L. O'Neill, *J. Med. Entomol.* **37**, 340 (2000).
- Materials and methods are available as supplementary materials on Science Online.
- S. L. Dobson, E. J. Marsland, W. Rattanadachakul, *Genetics* **160**, 1087 (2002).
- U. Tram, P. M. Ferree, W. Sullivan, *Microbes Infect.* **5**, 999 (2003).
- Z. Xi, J. L. Dean, C. Khoo, S. L. Dobson, *Insect Biochem. Mol. Biol.* **35**, 903 (2005).
- P. Lu, G. Bian, X. Pan, Z. Xi, *PLoS Negl. Trop. Dis.* **6**, e1754 (2012).
- X. Pan *et al.*, *Proc. Natl. Acad. Sci. U.S.A.* **109**, E23 (2012).
- C. M. Cirimotich *et al.*, *Science* **332**, 855 (2011).
- S. Kumar *et al.*, *Proc. Natl. Acad. Sci. U.S.A.* **100**, 14139 (2003).
- G. L. Hughes, A. D. Pike, P. Xue, J. L. Rasgon, *PLoS ONE* **7**, e36277 (2012).
- C. J. McMeniman, G. L. Hughes, S. L. O'Neill, *J. Med. Entomol.* **48**, 76 (2011).
- S. I. Hay *et al.*, *PLoS Med.* **7**, e1000209 (2010).
- M. E. Sinka *et al.*, *Parasit Vectors* **4**, 89 (2011).
- The malERA Consultative Group on Vector Control, *PLoS Med.* **8**, e1000401 (2011).
- R. E. Sinden, Y. Alavi, J. D. Raine, *Insect Biochem. Mol. Biol.* **34**, 625 (2004).
- Y. Dong *et al.*, *PLoS Pathog.* **7**, e1002458 (2011).

Acknowledgments: This work was supported by NIH grants R01AI080597, R21AI082141, and R01AI061576 and a

grant from the Foundation for the NIH through the Grand Challenges in Global Health Initiative of the Bill and Melinda Gates Foundation. We are grateful to the Johns Hopkins Malaria Research Institute Parasitology and Insectary Core Facilities and thank S. O'Neill, A. A. Hoffmann, and S. L. Dobson for their comments and suggestions and D. McClellan and S. Thiem for editorial assistance. Z.X. is also affiliated with Guangzhou WolbaKi Biotech Co., LTD. Data for this report are archived as supplementary materials on Science Online.

Supplementary Materials

www.sciencemag.org/cgi/content/full/340/6133/748/DC1
Materials and Methods
Figs. S1 to S3
Table S1
References (24–30)

6 February 2013; accepted 15 March 2013
10.1126/science.1236192

Delineating Antibody Recognition in Polyclonal Sera from Patterns of HIV-1 Isolate Neutralization

Ivelin S. Georgiev,^{1*} Nicole A. Doria-Rose,^{1*} Tongqing Zhou,^{1*} Young Do Kwon,^{1*} Ryan P. Staupé,¹ Stephanie Moquin,¹ Gwo-Yu Chuang,¹ Mark K. Louder,¹ Stephen D. Schmidt,¹ Han R. Altae-Tran,¹ Robert T. Bailer,¹ Krisha McKee,¹ Martha Nason,¹ Sijy O'Dell,¹ Gilad Ofek,¹ Marie Pancera,¹ Sanjay Srivatsan,¹ Lawrence Shapiro,^{1,2} Mark Connors,³ Stephen A. Migueles,³ Lynn Morris,^{4,5,6} Yoshiaki Nishimura,⁷ Malcolm A. Martin,⁷ John R. Mascola,^{1†} Peter D. Kwong^{1†}

Serum characterization and antibody isolation are transforming our understanding of the humoral immune response to viral infection. Here, we show that epitope specificities of HIV-1-neutralizing antibodies in serum can be elucidated from the serum pattern of neutralization against a diverse panel of HIV-1 isolates. We determined “neutralization fingerprints” for 30 neutralizing antibodies on a panel of 34 diverse HIV-1 strains and showed that similarity in neutralization fingerprint correlated with similarity in epitope. We used these fingerprints to delineate specificities of polyclonal sera from 24 HIV-1-infected donors and a chimeric simian-human immunodeficiency virus-infected macaque. Delineated specificities matched published specificities and were further confirmed by antibody isolation for two sera. Patterns of virus-isolate neutralization can thus afford a detailed epitope-specific understanding of neutralizing-antibody responses to viral infection.

Upon infection or vaccination, the adaptive immune system typically generates polyclonal antibody responses that recognize multiple epitopes (1–3). The serologic characterization of such polyclonal responses can inform vaccine design by elucidating which epi-

topes on the antigen are immunodominant and/or targets of pathogen-specific neutralizing antibodies. Such serologic analysis can further lead to the isolation of new monoclonal antibodies that may be of therapeutic value. As a result of extensive effort to understand the antibody response to viral infection, recent years have seen a surge in the isolation of monoclonal antibodies against HIV-1, influenza, hepatitis C, and other viruses (4–15). The link between polyclonal sera and component monoclonal antibodies, however, remains complex and difficult to decipher, in part, because of the extraordinary diversity of circulating antibodies. Viral genetic diversity can be an integral mechanism of immune evasion (16–22); this same diversity may, however, also provide a means by which to understand antibody responses (23, 24). Specifically, monoclonal antibodies targeting the same epitope on an antigen are likely to be affected in a similar way by diversity in that epitope region. When presented with a diverse set

of viral isolates, monoclonal antibodies may thus exhibit characteristic neutralization patterns or “neutralization fingerprints” (Fig. 1). Furthermore, neutralization patterns of a polyclonal serum could be viewed as the combined effect of the neutralization fingerprints of component monoclonal antibodies, and, if this relationship could be deconvoluted, then serum neutralization would serve as a predictor of component-antibody specificity.

To test this conjecture, we selected HIV-1 because of its high viral sequence diversity, the availability of well-characterized sera and antibodies, and the limited number of sites of vulnerability targeted by neutralizing antibodies on the HIV-1 spike (Env). These sites encompass the CD4-binding site (CD4bs), a variable loop V1/V2 site, and a glycan-V3 site on glycoprotein gp120, and the membrane-proximal external region (MPER) on gp41 (4–7, 13, 14, 25–35). The same site of vulnerability may encompass multiple epitopes and, as a result, can be targeted by antibodies with diverse specificities. To determine whether the neutralization fingerprints of HIV-1 monoclonal antibodies are a reflection of their epitope specificities, we utilized neutralization data for a panel of 34 diverse HIV-1 isolates (table S1), for 30 monoclonal antibodies recognizing diverse epitopes on HIV-1 Env, and for two variants of the CD4 receptor (table S2). Neutralization fingerprints for antibodies known to target similar epitopes correlated significantly better (Spearman correlation) than fingerprints of antibodies targeting different epitopes (fig. S1). On the basis of the neutralization-correlation values, antibodies were grouped into 10 clusters (Fig. 2A) (36), by using a clustering cutoff chosen to agree with known antibody structures and epitope-mapping (4–6, 13–15, 25–27, 37–40, 41). Two antibodies, 8ANC195 and HJ16, whose precise epitopes are currently unknown, clustered separately (5, 15), whereas all of the other antibody clusters could be mapped to known sites of Env vulnerability.

Overall, neutralization fingerprints appeared to exhibit sufficient specificity to successfully distinguish between antibodies targeting different

¹Vaccine Research Center, National Institute of Allergy and Infectious Diseases, National Institutes of Health, Bethesda, MD 20892, USA. ²Department of Biochemistry and Molecular Biophysics, Columbia University, New York, NY 10032, USA. ³Laboratory of Immunoregulation, National Institute of Allergy and Infectious Diseases, National Institutes of Health, Bethesda, MD 20892, USA. ⁴National Institute for Communicable Diseases, Sandringham 2131, South Africa. ⁵University of the Witwatersrand, Johannesburg 2001, South Africa. ⁶Centre for the AIDS Programme of Research in South Africa (CAPRISA), Durban 4013, South Africa. ⁷Laboratory of Molecular Microbiology, National Institute of Allergy and Infectious Diseases, National Institutes of Health, Bethesda, MD 20892, USA.

*These authors contributed equally to this work.

†Corresponding author. E-mail: jmascola@nih.gov (J.R.M.); pdkwong@nih.gov (P.D.K.)